

Confocal three dimensional tracking of a single nanoparticle with concurrent spectroscopic readouts

 Check for updates

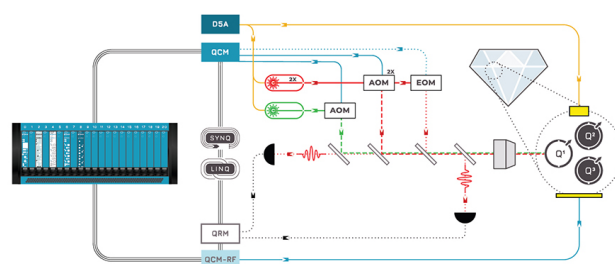
View
Online



Export Citation

Integrates all
Instrumentation + Software
for Control and Readout of

- Superconducting Qubits**
- NV-Centers**
- Spin Qubits**



NV-Centers Setup

find out more >

Confocal three dimensional tracking of a single nanoparticle with concurrent spectroscopic readouts

Hu Cang

Physical Biosciences Division, Lawrence Berkeley National Laboratory, Berkeley, California 94720

Chung M. Wong,^{a)} C. Shan Xu, and Abbas H. Rizvi^{b)}

Department of Chemistry, University of California at Berkeley, Berkeley, California 94720

Haw Yang^{c)}

Department of Chemistry, University of California at Berkeley, Berkeley, California 94720

and Physical Biosciences Division, Lawrence Berkeley National Laboratory, Berkeley, California 94720

(Received 31 October 2005; accepted 19 April 2006; published online 1 June 2006)

We present an apparatus that noninvasively tracks a moving nanoparticle in three dimensions while providing concurrent sequential spectroscopic measurements. The design, based on confocal microscopy, uses a near-infrared laser and a dark-field condenser for illumination of a gold nanoparticle. By monitoring the scattered light from the nanoparticle and using a piezoelectric stage, the system was able to continuously bring the diffusive particle in a glycerol/water solution back to the focal volume with spatial resolution and response time of less than 210 nm and a millisecond, respectively. © 2006 American Institute of Physics. [DOI: 10.1063/1.2204652]

Spectroscopic studies at the single-molecule or single-particle levels have provided invaluable information on the dynamics of complex systems that range in disciplinary fields from materials science to molecular cell biology.⁷ These measurements eliminate the confounding ensemble average and provides direct observation of the heterogeneity in space and time. To study long-term dynamics, a confocal or total internal reflection detection scheme is typically used in conjunction with immobilized molecular probes.¹ These widely used schemes, however, do not provide a means to capture the local dynamics on the nanometer scale in three dimensions (3D). Such knowledge constitutes the critical link between microscopic processes and macroscopic phenomena.

Real-time video tracking has been used in many applications for studying two dimensional movements. This popular technique, however, does not provide an accurate measurement along the system's optical axis, or in the *Z* direction. Indeed, it has been difficult to track a single moving particle in all three dimensions in real time. Several groups have proposed designs for following a particle in 3D with minimal perturbation. Peters *et al.*² elegantly used an overfilled detector to detect the *Z* position and a position sensor for the *X* and *Y* positions. Their method relies on a lensing effect of the diffusive polystyrene sphere, which sets a limit to the size of the bead by the diffraction limit of the light source and the difference in index of refraction between the bead and its surrounding medium. Levi *et al.*³ developed a clever scheme that excites a target particle with a nutating beam and determined the 3D position of the target by off-line demodulating the fluorescence signal. Their time resolution of 30–60 ms is dependent on the brightness of the particle

and the integration time. On the other hand, methods of similar spirit but actively trap small particles or single molecules have also been nicely demonstrated using, for instance, optical tweezers⁶ and two dimensional (2D) electrical field.^{4,5}

We propose that a confocal setup can form an intensity gradient for *Z*-axis resolution. This permits tracking of single nanoparticles with concurrent spectroscopic readouts, making it a general tool for 3D tracked single-molecule spectroscopy. Complementary to the active trapping approaches, this method is noninvasive and provides nanometer spatial resolution with submillisecond response time. In the present implementation, near-infrared (NIR) light scattered off a gold nanoparticle provides the feedback signal for tracking. This setup, however, should be capable of tracking fluorescence or photoluminescence from a single emitter, making it a general instrument. Illumination using NIR light has the following advantages when compared to using a visible light source: photoluminescence of the host material is reduced, greater penetration depth when working with turbid samples is achieved, photodamage of biological samples is minimized,⁸ and separation from the usual near-UV or visible excitation light is easily achieved by spectral filtering.

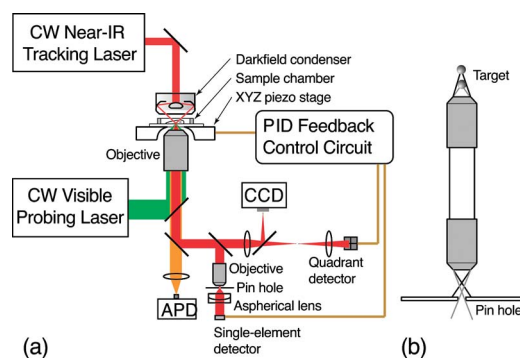


FIG. 1. (Color online) (a) Schematic diagram of the system. (b) The cartoon illustrates the principle of using a modified confocal setup to detect the movement of an object in the *Z* direction.

^{a)}Present address: Northrop Grumman Space Technology, Redondo Beach, CA 90278.

^{b)}Present address: Department of Molecular and Cellular Biology and Bauer Center for Genomics Research, Harvard University, Cambridge, MA 02138.

^{c)}Electronic mail: nawyang@berkeley.edu

Figure 1(a) outlines the experimental setup. The system is built around an inverted microscope (Olympus). NIR light from six 980 nm diode lasers (Fitel) is combined by a fiber coupler and expanded to fill a 0.65 numerical aperture (NA) dark-field condenser that focuses the NIR beam at the sample. The intensity of the laser beam is adjusted between 30 and 500 mW for best performance. The sample is placed on a 3D piezoelectric translation stage ($100 \times 100 \times 20 \mu\text{m}^3$, Physik Instrumente) with a no-load resonance frequency of 1.02 kHz at full swing. A 0.7–1.4 NA, $100\times$ infinity-corrected oil immersion objective lens (Leica) is placed beneath the sample. The scattered NIR light, collected by the objective lens, is split by a 50/50 beam splitter to an XY submodule and a Z submodule. The Z submodule has a $5 \mu\text{m}$ pinhole placed slightly behind the conjugate focal point of a 0.85 NA, $60\times$ objective lens. An aspheric lens collects all the light coming out of the pinhole and focuses it at an avalanche photodiode (OptoElectronic Components, OEC). Spatial resolution in the Z direction arises from the intensity gradient created by the throughput of light through the pinhole as the particle moves in and out of focus [Fig. 1(b)]. The light through the beam splitter forms an intermediate image by a 200 mm tube lens, and a second beam splitter reflects part of the light to a video camera for monitoring purposes. A 75 mm lens is placed before the quadrant avalanche photo diode (APD) (OEC) of the XY submodule. Using this two-stage setup, we achieve an overall magnification of $750\times$ for the XY submodule. The XY and Z signals from the two detectors are sent to a homemade analog feedback control circuit (corner frequency of 8.2 kHz) to control the 3D translation stage. For the spectroscopic probe, a 532 nm laser beam from a solid-state laser (Coherent) is coupled into the back aperture of the Leica objective lens through a long-pass dichroic mirror and focused at the sample. A second, short-pass dichroic mirror separates the NIR tracking light from the optical output of the green interrogation beam. The optical output is focused by a 180 mm tube lens in the microscope and detected by an APD (Perkin-Elmer).

The spatial and temporal responses of this system were first characterized using immobilized 250 nm gold colloid particles (Ted Pella) spin coated on a glass cover slip. In these experiments, a particle was selected by using the video camera and a joystick to steer a particle into the focal region. Upon engaging the feedback circuit, the XY submodules attempt to minimize the quadrant APD signal by driving the stage to center the particle at the focus while the Z submodule latches onto the intensity signal and finds a position where the particle movement would produce the largest intensity gradient at the photodiode. This sequence of events is depicted in Fig. 2. As shown in the figure, the response time is less than $500 \mu\text{s}$ in both the X and the Y directions. The Z positioning being sensitive to fluctuations in X-Y positioning was improved by turning on the Z feedback after the X-Y positioning stabilized. The transient of the X and Y channels decays within 1 ms. However, that of the Z channel takes several milliseconds to decay out. The performance could be tuned by adjusting the proportional-integral-derivative (PID) parameters. The histograms of the fluctuations in the X, Y, and Z directions are shown on the side of Fig. 2 where the standard deviations were determined as 10, 14, and 34 nm, respectively, caused mainly by a combination of electronic and mechanic fluctuations. After closing the feedback loop,

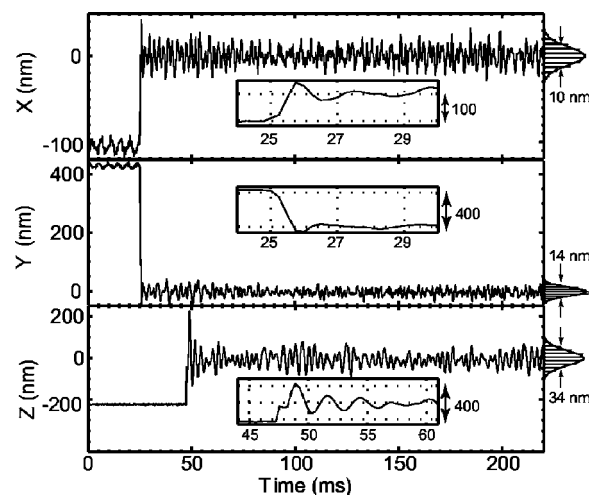


FIG. 2. Typical stage positions in the X, Y, and Z directions as a function of time. The standard deviations are shown on the side. The insets zoom in at the first several millisecond trajectories just before and after the feedback engages.

the oscillations became slightly more pronounced as the controllers attempt to bring the particle back to the focal volume under the influence of the electronic and mechanic noises.

We then tested our system on a moving particle and demonstrated simultaneous single-particle tracking and spectroscopic readouts. In this experiment, a second green laser was used to interrogate the tracked particle. As a proof of principle, the backscattered light of the green beam was taken as the spectroscopic optical readout. The sample, consisted of a drop of 3% (v/v) water in glycerol solution containing dilute 250 nm gold particles, was sandwiched between two cover slips with the edges sealed with wax to prevent leakage. We intentionally studied particle movements under nonequilibrium conditions to illustrate its use in studying cases beyond simple Brownian motion. To do so, we nudged the sample to create a sheared flow and took the data before the sample reequilibrated.

The intensity time trace of the backscattered green light, fluctuating around a nonzero value, is shown in Fig. 3(a). With negligible laser noise, the variation in the green light intensity is due to the fluctuation in the positioning of the particle. Figure 3(b) shows the histogram of the green light intensity trajectory, with the abscissa normalized by the maximum photon count and the ordinate normalized by the total number of data points in the trajectory. The histogram exhibits a bell shape centered just below 0.5. This indicates that the green light focal point deviates from the tracked origin by Δ . At the focal point, the green light is assumed to exhibit a Gaussian profile. For a confocal setup, the detected green light intensity becomes $I(r, z) \propto \exp[-2r^2/(1$

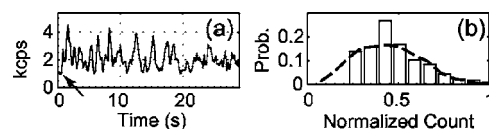


FIG. 3. (a) The scattered green light intensity measured by an APD. The arrow indicates the time instance when the tracking mechanism is engaged. (b) A histogram of the green light intensity. The deviation of the maximum position from 1 corresponds to the difference, Δ , between the green light focus point and the tracking origin, and the width indicates the standard deviations σ_x , σ_y , and σ_z .

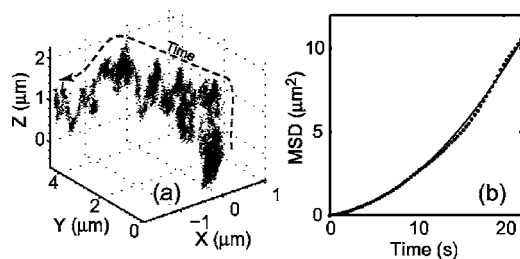


FIG. 4. (a) The 3D trajectory of a 250 nm gold particle obtained by measuring the counter movement of the translation stage. For clarity, only every ten points are shown here. (b) The mean square displacement of the particle from the origin is plotted as a function of time. The solid line is a fit to a mixed diffusive and directional motion.

$+z^2/z_R^2)/w_0^2]$, where r and z are the in-plane and axial distances from the focus, w_0 is the waist, and z_R is the Rayleigh range. Assuming also that the particle positioning has a Gaussian distribution in space as $f(r, z) = N \exp[-(x - \Delta)^2/2\sigma_x^2 - (y - \Delta)^2/2\sigma_y^2 - (z - \Delta)^2/2\sigma_z^2]$, where N is the normalization factor, σ_x , σ_y , and σ_z are the standard deviations, and Δ is the deviation between the green light focus and the tracked origin which we assumed to be equal in all three directions for the purpose of simplicity. Using $\sigma_x = 65$ nm and $\sigma_y = 116$ nm obtained from video tracking, we obtain the upper limit of $\sigma_z \sim 210$ nm and $\Delta \sim 180$ nm. Since the Z position is not decoupled to the X - Y sensing in this implementation, its performance is somewhat degraded.

The 3D position of the particle was deduced from the stage movement through its built-in capacitive sensor and digitized every 333 μ s as shown in Fig. 4(a). The nonequilibrium condition of the sample is indicated by the directional flow along the Y direction. The mean velocity can be estimated using the mean-square-displacement (MSD) plot in Fig. 4(b). For a combined diffusive and flow motion, the MSD is equal to $\text{MSD}(t) = 6Dt + (vt)^2$.³ The fit shown in Fig. 4(b) as a solid line gives $D = 0.013 \mu\text{m}^2/\text{s}$ and $v = 0.13 \mu\text{m}/\text{s}$. Using the Stokes-Einstein relation, the corresponding viscosity of the solution is $\eta = 130$ cP, which corresponds to a 2.4% concentration of water by volume deduced from Raoult's law. This result is very close to the 3% real concentration.

The tracking light may introduce undesirable heating and trapping in this configuration. Mie scattering theory shows that a 250 nm gold particle has an absorption cross section of $\Sigma_{\text{abs}} = 0.0047 \mu\text{m}^2$ at 980 nm. For a focal spot radius of the dark-field condenser of $r \approx 11 \mu\text{m}$ and input

power of about $P = 100$ mW, the amount of power absorbed by the particle is $P_{\text{abs}} \sim P \Sigma_{\text{abs}} / \pi r^2 = 0.0012$ mW. Assuming the steady state condition $P_{\text{abs}} = \kappa 4 \pi R^2 dT/dR$, where κ is the thermoconductivity of water, we calculated a small difference in temperature of $\Delta T \sim 1.3$ K. For a smaller particle, ΔT will be even smaller. Since the illumination spot by the dark-field condenser is broad with a full width at half maximum of 11 μm , the gradient of the intensity profile produces negligible trapping force. To estimate the upper-limit response time of our design, we consider the worst-case scenario in which the sample chamber is not sealed such that the particle is counteracted by stage movement-induced shearing. In this case, there will be a time delay t between the stage and the particle movement. By the Navier-Stokes equation, the shearing propagates a distance of $\sqrt{2(\eta/\rho)t}$ in t , where ρ is the density of the fluid. Using water's η and ρ , we estimate that it takes about 50 μs for the shearing to propagate from the coverglass to a particle 100 μm above it. This is much faster than that of the stage and can be neglected.

In summary, we have demonstrated a method that continuously follows the position of a single nanoparticle in 3D and provides real-time sequential spectroscopic information of the particle. As a proof of principle, we have shown that a 250 nm gold particle can be maintained at the focus of a tightly focused green laser beam for a prolonged period (minutes). The scattered green light remains relatively flat comparing to short bursts as one would have obtained in a diffusing single-molecule experiment. Our apparatus holds great promise in applying single-molecule spectroscopy and imaging on a nonstationary target.

This work was supported by the Office of Science, U.S. Department of Energy under Contract No. DE-AC03-76SF00098, by the University of California at Berkeley, and by the Hellman Family Faculty Fund. H. Chang is acknowledged for assistance in procurement.

¹P. Tinnefeld and M. Sauer, *Angew. Chem., Int. Ed.* **44**, 2642 (2004).

²I. M. Peters, B. G. de Grooth, J. M. Schins, C. G. Figdor, and J. Greve, *Rev. Sci. Instrum.* **69**, 2762 (1998).

³V. Levi, Q. Ruan, and E. Gratton, *Biophys. J.* **88**, 2919 (2005).

⁴A. E. Cohen, *Phys. Rev. Lett.* **94**, 118102 (2005).

⁵A. E. Cohen and W. E. Moerner, *Appl. Phys. Lett.* **86**, 093109 (2005).

⁶M. J. Lang, P. M. Fordyce, A. M. Engh, K. C. Neuman, and S. M. Block, *Nat. Methods* **1**, 1 (2004).

⁷W. E. Moerner and D. P. Fromm, *Rev. Sci. Instrum.* **74**, 3597 (2003).

⁸K. C. Neuman, E. H. Chadd, G. F. Liou and S. M. Block, *Biophys. J.* **77**, 2858 (1999).